Research Article

Journal of Environmental Nanotechnology

Microwave Synthesis of Triethanolamine-doped Zinc Oxide Nanoparticles

J. Nancy, V. Kalaiselvi*, B. Blessymol, P. Yasotha, M. Vishalatchi, S. Pavithra

Department of Physics, Navarasam Arts and Science College for Women, Erode, TN, India

Received: 29.04.2022 Accepted: 05.05.2022 Published: 30-06-2022

*nk.arthi.kalai@gmail.com

ABSTRACT

In this work, Triethanolamine-doped Zinc Oxide (ZnO) nanoparticles were synthesized by chemical deposition, associated with the microwave irradiation method. The synthesized zinc oxide nanoparticles were characterized by Scanning Electron Microscope, X-Ray Diffraction, Fourier Transform Infrared Spectroscopy, Ultra Violet - visible spectroscopy, Photo Luminescence Spectroscopy and Antimicrobial Activity. The prepared sample's surface morphology, crystalline size, functional groups, absorbance and band gap, and emission wavelength were calculated. Antimicrobial activity was performed to predict the zone of inhibition of synthesized nanoparticles.

Keywords: Triethanolamine; Zinc oxide; Absorbance; Emission wavelength; Inhibition.

1. INTRODUCTION

Nanotechnology is the technology implemented at the Nanoscale of range 1-100 nm in size (Karthika *et al.* 2021). It plays a very important role in modern research and is also applied in pharmaceuticals, cosmetics, electronics, health care, biomedical science, drug and gene delivery, chemical industry, environment, health, space, and industries (Nandhini *et al.* 2020). Nanoparticles can be synthesized by using the top-down approach and bottom-up approach. Zinc (Zn) is the most widely used metal with a low melting point and density of 1.84 g/cm^3. Zinc oxide is a white, powdery mineral used for sun protection (Pavithra *et al.* 2020; Hassellov *et al.* 2008). Triethanolamine is a viscous organic compound that is both a tertiary amine and a triol. Triethanolamine is used as a surfactant and an agent for reducing the surface tension between two media, as well as for dry cleaning and cosmetics, and as a general emulsifier for preparations (Caleb Abiodun Popoola *et al.* 2015; Rajalakshmi *et al.* 2000).

2. MATERIALS AND METHODS

2.1 Materials

The chemicals like Zinc acetate dehydrate, Triethanolamine, distilled water and Sodium Hydroxide pellets were purchased from Erode, Tamilnadu, India.

2.1 Synthesis of Triethanolamine-doped Zinc Oxide Nanoparticles

Triethanolamine-doped Zinc Oxide nanoparticles were synthesized by microwave irradiation method. In this work, 1 ml of Triethanolamine (TEA) solution was mixed with 250 ml of distilled water and stirred for 30 minutes. Then, 7 grams of zinc acetate dehydrate was added to the above mixture and again stirred for 30 minutes using a magnetic stirrer. 4 grams of NaOH solution was added drop by drop to the prepared solution to maintain its pH at 12. The mixture was stirred again for half an hour. The synthesized sample was aged for 24 hours. After 24 hours, a white color precipitate was obtained. It was kept in a microwave oven at 75 W for 30 minutes and calcinated in a muffle furnace at 400 °C for 4 hours. Finally, the prepared sample was mortared and fine powder of nanoparticles were obtained (Kolodziejczak Radzimsk and Jesionowski, 2014).

3. CHARACTERIZATION TECHNIQUES

3.1 SEM Analysis

The Scanning electron microscope (SEM) technique uses a narrow electron beam to collect high-resolution, high-magnification images of back-scattered electrons from sample surfaces. Due to the narrowness of the excitation beam, the resultant images have a high depth-of-field that can be used to understand particle topography.

3.2 XRD Analysis

The prepared samples were analyzed using XRD (X-ray Diffraction) technique. This XRD pattern predicts the lattice parameters (a and c), unit cell volume and crystalline size of the sample. The XRD pattern of prepared samples was well-matched with JCPDS file. The lattice parameters of the sample were calculated using the following equation:

$$1/d^2 = (4(h^2+hk+k^2)/3a^2) + (1^2/c^2))$$

where, d is the spacing between the planes, and a and c are the lattice parameters.

The unit cell volume (V) of the sample is given by:

$$V = (\sqrt{3}/2) + a^2 + c^2$$

The sample's average crystalline size was determined using Scherer's formula:

$$D = K\lambda/\beta \cos\theta$$

where, D denotes the average crystalline size of the sample, K represents the broadening constant, λ denotes the wavelength of CuKα radiation source (1.54 Å), β represents the full width at half maximum and θ denotes the angle of diffraction.

3.3 FTIR Analysis

FTIR (Fourier transform spectroscopy analysis) is an analytical methodology used in industry and academic laboratories to understand the structure of individual molecules and the composition of molecular mixtures (Karthika *et al.* 2021).

3.4 UV Analysis

UV-Vis. Spectroscopy (or Spectrophotometry) is a quantitative technique to measure how much a chemical substance absorbs light. This technique can be used for multiple samples, including liquids, solids, thin films and glass.

3.5 PL Analysis

Photoluminescence (PL) is an optical phenomenon in which semiconductors give light emissions by absorbing incident light whose energy is higher than the energy band gap of the semiconductor. In the mechanism of PL, the excited electrons generated by optical excitation will return to the ground state, accompanied by emitting photons.

3.6 Antimicrobial Activity

Antibacterial activity was studied for the prepared powder sample against the gram-positive cocci *Staphylococcus Aureus* and gram-negative bacilli *Escherichia Coli* by the Agar well diffusion method. The good size of 6.0 mm was made and grown in Muller Hinton Agar in a 90 mm plate. The standardized inoculums are inoculated in the plates prepared aseptically earlier by dipping a sterile in the inoculums. The excess was removed by passing, pressing and rotating the swab 3 times at an angle of 60º C. The swab was passed around the edge of the agar surface. The lids were left closed and made to dry at room temperature. The petri dish was divided into two parts; in one part 100 µg sample disc was placed and 10 µg of standard Ciprofloxacin was placed in another by sterile forceps. The setup was kept in a refrigerator at 4º C for diffusion and incubated at 37 ºC for 24 hours. The zone of inhibition produced by the sample was observed and measured using a scale and record the average of the two diameters of each zone of inhibition was recorded.

4. RESULTS AND DISCUSSION

4.1 X-RAY Diffraction Analysis

XRD analysis determines the crystalline nature and phase identification of the nanoparticles. XRD is primarily used for phase identification of a crystalline material and can provide information on unit cell dimensions. The XRD pattern of prepared TEA-doped ZnO is shown in Fig. 1. The diffraction peaks of TEA-doped ZnO at 2θ = 31.96, 36.46, 47.67, 56.74 and 66.50 were identified. The indexed hkl planes were (100), (101), (102), (110) and (200). The average crystalline size (D) of TEA-doped ZnO was 46.88 nm. The unit cell volume (V), lattice parameters a and c decreased due to an increase in crystalline size, as shown in Table 1. The prepared sample confirms the hexagonal structure and is well-matched with JCPDS files. No impurity peaks were detected.

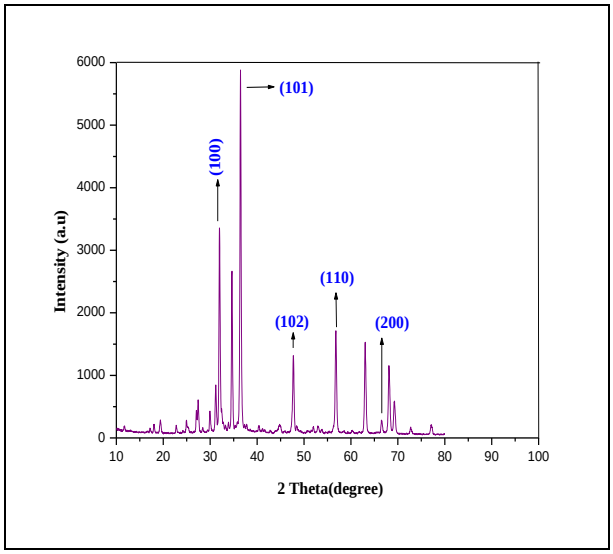

Fig. 1: XRD pattern for TEA-doped ZnO.

Table 1. XRD Analysis

Sample	2θ (deg)	FWHM (deg)	D (A°)	Crystalline size (nm)	Average Crystalline size (nm)	hkl	Lattice Constant		Unit Cell Volume (V)
							a=b	c	
TEA-ZnO	31.96	0.2175	2.8002	38.13	46.88	100	3.19	5.17	45.76
	36.46	0.2342	2.4643	35.72		101			
	47.67	0.1004	1.9074	86.51		102			
	56.74	0.2342	1.6224	38.56		110			
	66.50	0.2676	1.4059	35.51		200			

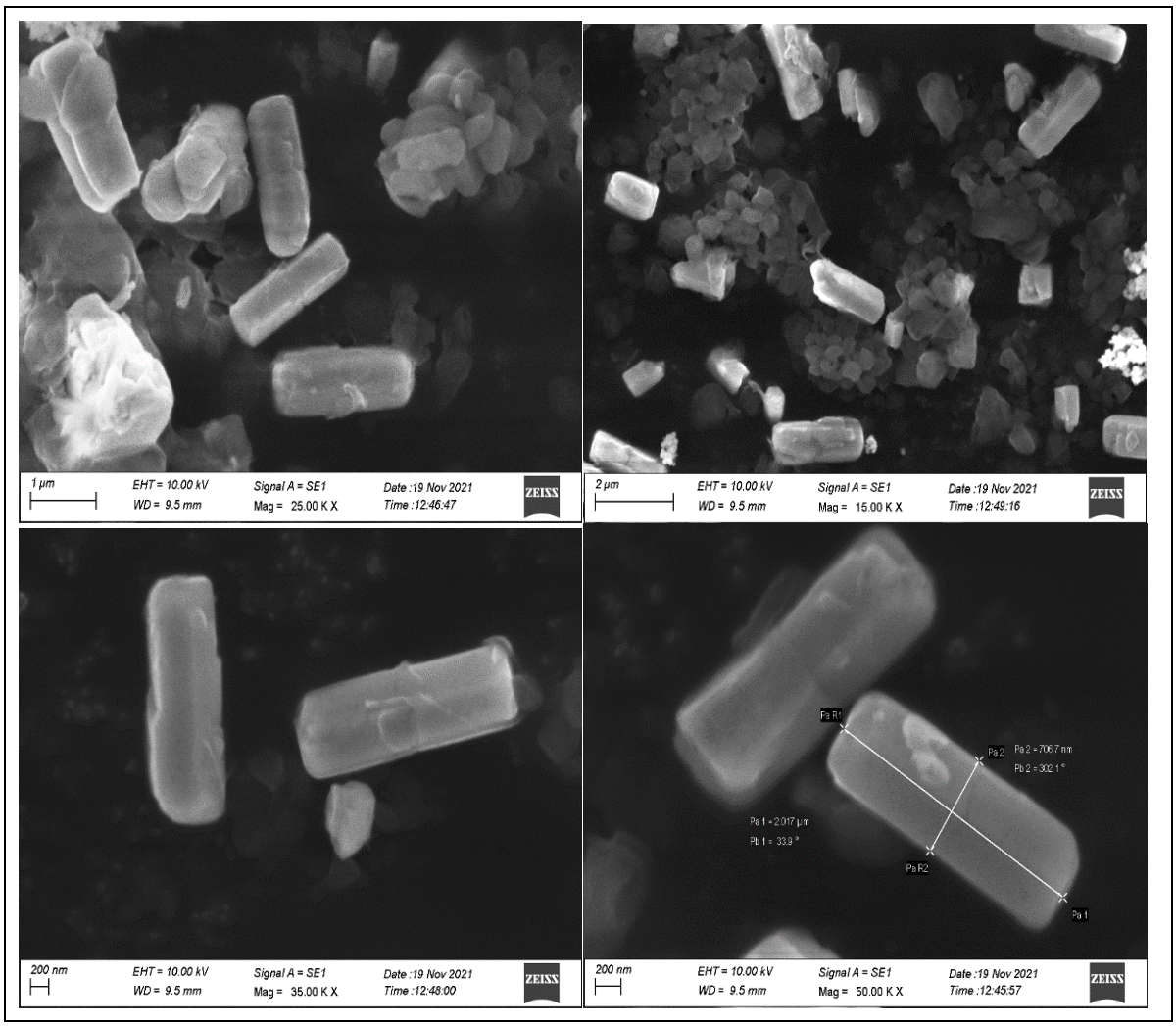

Fig. 2: SEM analysis for TEA-doped ZnO.

4.2 SEM Analysis

The morphologic structure of the prepared nanocomposites was revealed in SEM analysis. Fig. 2 shows the cylindrical rod-shaped structure of Triethanolamine-doped Zinc Oxide.

4.3 FTIR Analysis

The Fourier transform infrared spectroscopy of TEA-doped ZnO nanoparticles was done. FTIR is used to investigate the functional elements in the synthesized nanoparticles. Fourier Transform Infrared Spectroscopy (FTIR) identifies chemical bonds in a molecule by producing an infrared absorption spectrum. The prepared TEA and doped-ZnO samples' FTIR spectra were plotted between the wavelength ranges of about 4000-500 cm^{-1}, as shown in Fig. 3. The peaks were observed in different wave numbers. A large absorption peak at 3418.55 cm^{-1} corresponds to the N-H stretching. The peaks at 2991.34 cm^{-1} and 1558.48 cm^{-1} represent O-H stretching bonded and the N-H in-plane bending, respectively. The peak at 1411.89 cm^{-1} corresponds to COO-symmetric stretching, and 1010.70 cm^{-1} represents the CH in-plane bending. The absorption peaks at 928.12 cm^{-1} indicate the presence of C-O-C stretching, and the peak at 794.67 cm^{-1} represents the C-H bending. And then, OCN deformation represented the peak at 640.37 cm^{-1}, respectively. Those results indicate that the synthesized ZnO nanoparticles were stabilized by chemical molecular constituents present in the Triethanolamine-doping particles, as shown in Table 2.

Table 2. FTIR functional group of TEA-doped ZnO.

S. No.	Wave number (cm^{-1})	Intensity	Stretching vibration
1.	2991.34	Week	OH stretching (bonded)
2.	3418.55	Medium-Week	N-H stretching
3.	1558.48	Strong	N-H in-plane bending
4.	1411.89	Strong	COO^- symmetric stretching
5.	1010.70	Week (sharp)	C-H in-plane bending
6.	918.12	Medium	C-O-C stretching
7.	794.64	Week	C-H bending
8.	640.37	Medium	OCN deformation

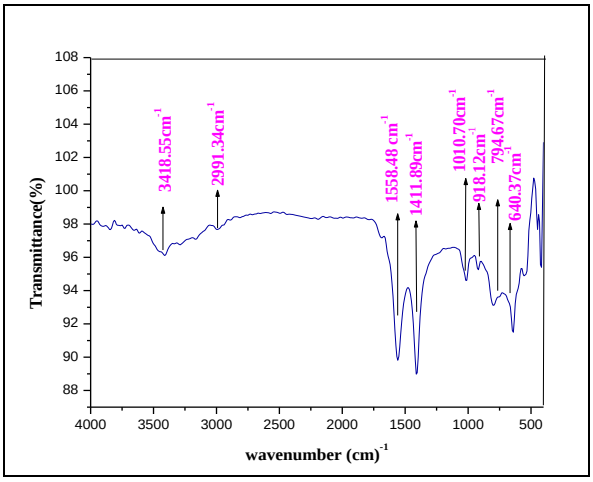

Fig. 3: FTIR Spectrum of TEA-doped ZnO.

4.4 UV-Vis. Spectroscopy Analysis

UV-Vis. spectrum of TEA-doped ZnO nanoparticles is shown in Fig. 4. The spectrum was recorded in the range of 200-900 nm. Samples are exhibiting the absorbance peak in the UV region. The band gap energy of the sample can be predicted by the given formula $Eg = hc/\lambda$. The absorption wavelength of TEA-doped ZnO was 366 nm and the band gap energy was 3.19 eV. The band gap energy is shown in Table 3.

Table 3. UV-Vis. spectrum of TEA-doped ZnO.

Sample Name	Wavelength (nm)	Band Gap Energy (eV)
TEA	366	3.19

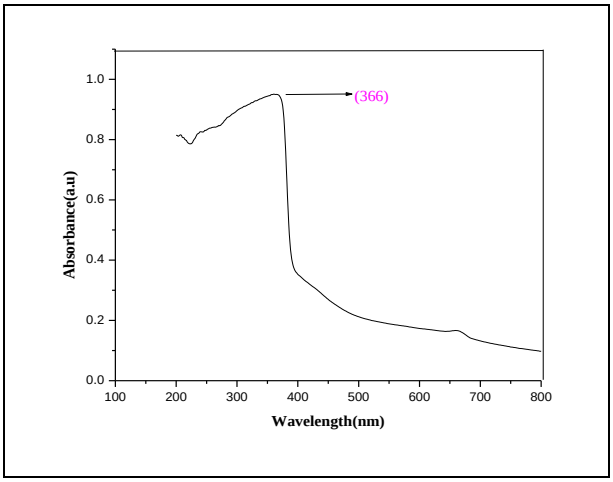

Fig. 4: UV-Vis. spectrum of TEA-doped ZnO.

4.5 Photoluminescence Spectroscopy

The intensity of emission radiations was absorbed by photoluminescence spectroscopy. The emission radiation of TEA-doped ZnO is shown in Fig. 5. The excitation wavelength occured at 83.56 nm for TEA-doped ZnO nanoparticles.

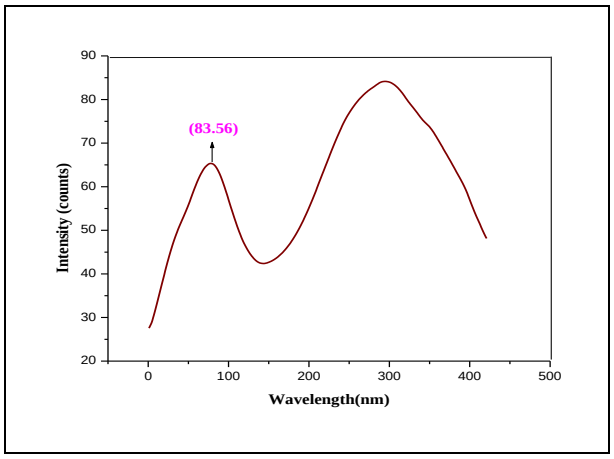

Fig. 5: PL Analysis for TEA-doped ZnO nanoparticles.

Table 4. Zone of inhibition of TEA Nanoparticles.

Sample name	Zone inhibition (mm)			
	Gram-positive		Gram-negative	
	Bacillus	*Staphylococcus*	*E. Coli*	*Pseudomonas*
TEA (ZnO)	21	22	16	21

4.6 Antimicrobial Activity

The Anti-bacterial of TEA-doped ZnO was studied against gram-positive bacteria of *Bacillus* and *Staphylococcus*, gram-negative bacteria of *E. coli* and *Pseudomonas* by Agar well diffusion method. The antibacterial of TEA-doped ZnO are displayed in Fig. 6, and the values are given in Table 4. The zone of inhibition for gram-positive bacteria against *Bacillus* and *Staphylococcus* was 21 mm and 21 mm for TEA. The gram-negative bacteria against *E. Coli* and *Pseudomonas* have a zone of inhibition of 16 mm and 21mm for TEA. The prepared TEA samples were effective.

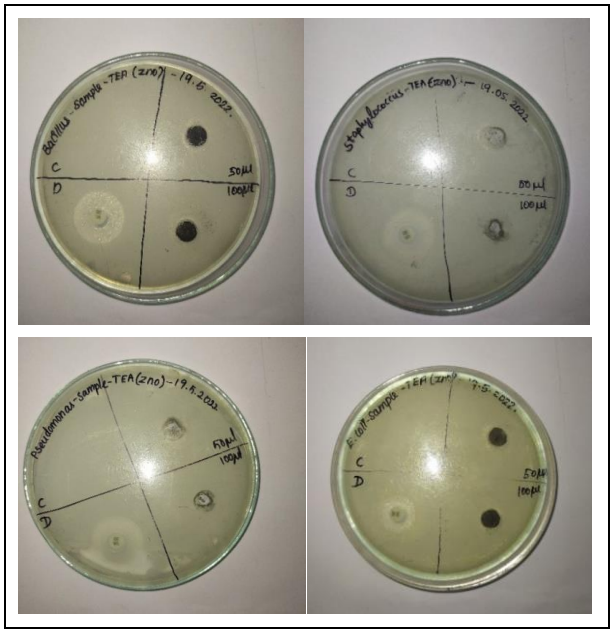

Fig 6: Antimicrobial Activity.

5. CONCLUSION

The zinc oxide nanoparticles were synthesized using the doping agent Triethanolamine in this work. The successful formation of Zinc Oxide nanoparticles was confirmed by XRD, SEM, FTIR, UV, PL and Antimicrobial Activity.

- XRD pattern had confirmed the presence of hexagonal structure and it was used to determine the crystalline size of the Triethanolamine-doped Zinc oxide sample and its unit cell dimensions.
- SEM had shown the morphological structure of the prepared sample. Furthermore, it gave the rod shapes for Triethanolamine-doped Zinc oxide.
- The FTIR analysis had shown the different functional groups present in the sample.
- UV-Vis. spectrum had shown the bandgap energy and wavelength for TEA-doped ZnO. The band gap energy of Triethanolamine-doped Zinc oxide was 3.19 eV.
- PL analysis revealed the optical properties of the prepared sample.
- Antimicrobial activity predicted the zone of inhibition from 16 mm to 21 mm. The prepared Triethanolamine-doped Zinc oxide sample was effective.

FUNDING

This research received no specific grant from any funding agency in the public, commercial, or not-for-profit sectors.

CONFLICTS OF INTEREST

The authors declare that there is no conflict of interest.

REFERENCES

Caleb Abiodun Popoola, Jerome Adekunle Ayo, Olajide Emmanuel Adedeji and Ogungbemi Akinleye, TEA as flow improver for heavy crude oils, *IOSR J. Appl. Phys.*, 8(3), 34-38 (2015). https://doi.org/10.9790/5736-08313438

Hassellov, M., Readman, J.W., Ranville, J.F. and Tied, K., Nanoparticle analysis and characterization methodologies in environmental risk assessment of engineered nanoparticles, *Ecotoxicol.*, 17(5), 344-361 (2008). https://doi.org/10.1007/s10646-008-0225-x

Karthika, V., Ramya, V., Kalaiselvi, V. and Shanmathi, S., Zinc oxide nanoparticles synthesis and characterization using justiciaadhatoda leaf extract, *Int. J. Adv. Sci. Eng.*, 7(3), 1839-1842 (2021). https://doi.org/10.29294/IJASE.7.3.2021.1839-1842

Kolodziejczak Radzimsk, A, and Jesionowski, T., Zinc Oxide–from synthesis to application: a review, *Mater.*, 7(4), 2833-2881 (2014). https://doi.org/10.3390/ma7042833

Nandhini, P., Surya, K., Kalaiselvi, V., Ramya, V. and Vidhya, N., Synthesis and characterization of pure and capped zinc oxide nanoparticles using nigella sativa, *Int. J. Adv. Sci. Eng.*,7(2), 1756-1760 (2020). https://doi.org/10.29294/IJASE.7.2.2020.1756-1760

Pavithra, S., Sudha, P., Kalaiselvi, V., Ramya, V., Vidhya, N., Green synthesis and characterization of zno nanoparticles using hibiscus rosa sinensis leaf extract, *J. of Environ. Nanotechnol.*, 9(3), 7-12 (2020). https://doi.org/10.13074/jent.2020.09.203419

Rajalakshmi, M, Arora, A.K., Bendre, B.S. and Mahamuni, S., Optical phonon confinement in zinc oxide nanoparticles, *J. Appl. Phys.*, 87(5), 2445-2448 (2000). http://dx.doi.org/10.1063/1.372199